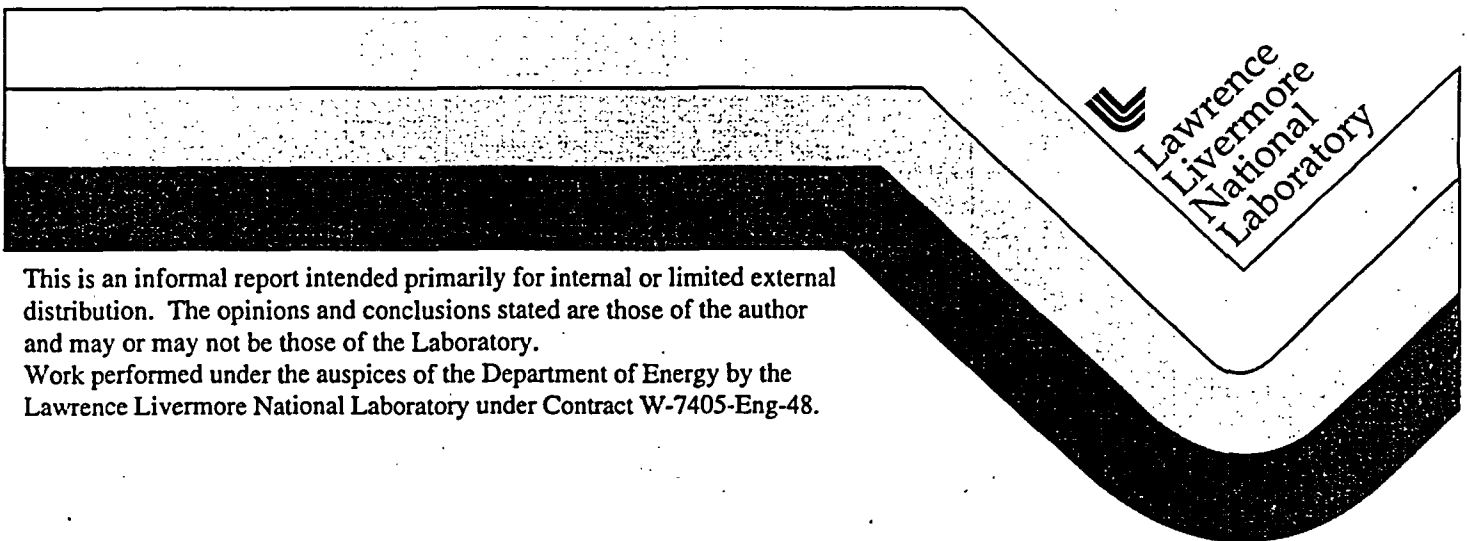


Capillary Barriers: Bench-top Laboratory Experiments and Numerical Modeling

Dorthe Wildenschild
Nina D. Rosenberg

September 16, 1999



This is an informal report intended primarily for internal or limited external distribution. The opinions and conclusions stated are those of the author and may or may not be those of the Laboratory.

Work performed under the auspices of the Department of Energy by the Lawrence Livermore National Laboratory under Contract W-7405-Eng-48.

DISCLAIMER

This document was prepared as an account of work sponsored by an agency of the United States Government. Neither the United States Government nor the University of California nor any of their employees, makes any warranty, express or implied, or assumes any legal liability or responsibility for the accuracy, completeness, or usefulness of any information, apparatus, product, or process disclosed, or represents that its use would not infringe privately owned rights. Reference herein to any specific commercial product, process, or service by trade name, trademark, manufacturer, or otherwise, does not necessarily constitute or imply its endorsement, recommendation, or favoring by the United States Government or the University of California. The views and opinions of authors expressed herein do not necessarily state or reflect those of the United States Government or the University of California, and shall not be used for advertising or product endorsement purposes.

This report has been reproduced
directly from the best available copy.

Available to DOE and DOE contractors from the
Office of Scientific and Technical Information
P.O. Box 62, Oak Ridge, TN 37831
Prices available from (615) 576-8401, FTS 626-8401

Available to the public from the
National Technical Information Service
U.S. Department of Commerce
5285 Port Royal Rd.,
Springfield, VA 22161

Work performed under the auspices of the U.S. Department of Energy by Lawrence Livermore National Laboratory under contract W-7405-ENG-48. This work is supported by Yucca Mountain Site Characterization Project, LLNL.

Capillary Barriers: Bench-top Laboratory Experiments and Numerical Modeling

D. Wildenschild¹ and N. D. Rosenberg²

¹**Geophysics & Global Security Division**
²**Geosciences & Environmental Technologies Division**
Earth and Environmental Sciences Directorate
Lawrence Livermore National Laboratory
Livermore, CA 94551.

September 16, 1999

Abstract

Capillary barriers typically consist of two layers of granular materials designed so that the contrast in hydrologic properties and sloping interface between the layers keeps infiltrating water in the upper layer. We report here on the results of two bench-top capillary barrier experiments, identical except for the coarse material used in the lower layer. These experiments were conducted to better understand the behavior of capillary barriers as they might be used in an engineered barrier system at the potential high-level nuclear waste site at Yucca Mountain.

We measured hydrologic parameters for both coarse materials using typical methods and found that both materials, although morphologically different (rounds vs. angular), had very similar hydrologic properties. The rounded sand provided a better functioning capillary barrier than the angular sand, but neither experiment was a perfectly working capillary barrier. Water infiltrated the lower coarse material in both our experiments. In both cases, however, over 93% of the infiltrating water was successfully diverted from the lower layer.

Our experimental results show that prediction of capillary barrier performance based on standard hydrologic property measurements is not always adequate to predict system behavior. Moreover, our numerical simulations of these experiments showed that predicted capillary barrier performance was very sensitive to small changes in model hydrologic parameter values, within the likely uncertainty and variation of these values in this case. We believe these are important points to consider with respect to capillary barrier design.

Table of Contents

	page
Abstract.....	i
Introduction	1
Laboratory Experiments.....	2
Methodology	2
Hydrologic Properties.....	3
Experimental Results	3
Modeling Studies.....	5
Description of Numerical Model.....	5
Model Results.....	5
Discussion and Conclusion	6
References	6

Introduction

Capillary barriers are well-described by Oldenburg and Pruess (1993):

A capillary barrier forms in unsaturated conditions when a fine layer overlies a coarse layer. The barrier arises from the difference in effective liquid permeability between the fine layer and the coarse layer in unsaturated conditions. As infiltration from above accumulates in the fine soil at the contact, the liquid saturation (S_l) increases in the fine layer and the capillary pressure becomes less negative. The absolute permeability of the fine layer is smaller, so at some value of S_l below unity, the effective permeability of the fine and coarse soils will be equal. If the contact between the fine and coarse layers is horizontal, the moisture will build up in the fine layer until the permeability difference becomes sufficiently small that the capillary barrier will fail and water will enter the coarse layer. If the contact between the two layers is tilted, the moisture which builds up will be diverted and will flow along the contact within the fine layer as capillary diversion.

The functioning of capillary barriers involves two coupled processes: (1) the exclusion of infiltration from the coarse layer; and (2) the diversion within the fine layer of excluded infiltration down-dip above the contact. Thus capillary barriers rely on contrasting hydraulic properties between the two layers for the exclusion part of the process and on the dip and permeability of the fine layer for the diversion part of the process. The coupling arises because the exclusion of water from the lower layer is a function of capillary pressure and relative permeability, which are functions of liquid saturation.

About one year ago, the Engineered Barrier Systems Operations (EBSO) group of the Yucca Mountain Project began investigating the possibility of including a capillary barrier in the Engineered Barrier System (EBS) at the potential Yucca Mountain nuclear waste repository site. We were asked by EBSO to participate in this effort.

Although engineered capillary barriers are widely used to minimize infiltration into large shallow landfills, the issues involved with using engineered capillary barriers to limit water contact with contaminant sources at the potential high-level nuclear waste site at Yucca Mountain are very different. These issues include: shorter required diversion path length (the current design calls for disposal tunnels about 5 m in diameter), longer temporal scale, and more stringent performance goals.

Another issue is the effect of thermohydrologic processes that would occur in a system with elevated repository temperatures and steep temperature gradients. These conditions result in two-phase flow processes such as evaporation and condensate formation, and could result in the backfill materials being altered from that of the as-placed material, changing hydrologic properties in a way that changes the performance of the EBS system.

The experiments reported here were originally planned as the first phase of an investigation designed to assess the effects of thermohydrologic (and thermohydrologic-chemical) processes on the performance of a capillary barrier system. The first phase of this activity was to conduct bench-top tests under ambient conditions as a base case for comparison. Due to changing YMP priorities, this project was terminated before the completion of this first phase. This report documents the experimental methods and results to date, with limited analysis and modeling.

Laboratory Experiments

Methodology

All the reported experiments were carried out as bench-top laboratory experiments using an aluminum box of dimensions 60.5 cm x 56.0 cm x 10 cm with a Pyrex window on one side allowing easy detection of flow patterns, Figure 1. The box was designed to withstand temperatures ~100 °C. Two 0.5-bar tensiometers were installed from the backside of the box (marked as squares in Figure 1). The tensiometers consisted of porous ceramic cups glued onto the backside of the box and they were tested to have an air-entry value of at least 250 cm prior to use. Drainage out of the box was achieved by use of two stainless steel sintered rods installed from the backside immediately above the fine/coarse interface (circles in Figure 1). These drains had relatively low air-entry values (< 70 cm), but were highly permeable. They were connected to water-filled tubing, which was hanging off the bench-top, thus providing water-phase tension to facilitate drainage under less than fully saturated conditions. Initially, a 5 cm by 10 cm porous plate, mounted on the side of the box at the fine/coarse interface, was used for drainage, but persisting problems with this plate prompted the installation and use of the highly permeable sintered rods. The porous plate did, however, function as an additional tensiometer in some of the experiments. Temperature variations during the experiments were measured with four thermocouples (1.02 mm diameter) placed in the box as shown in Figure 1 (stars).

The sandy materials were packed loosely in the box to simulate the emplacement in the waste drifts obtained when using a conveyor belt. Before the materials were poured into the box, it was tilted (using a crane) to a 24° angle so that the fine/coarse interface was horizontal. All the material was weighed so that individual porosities of the two materials could be determined. The porosities of the two experiments reported here are listed in Table 1 along with other relevant information for each experiment.

An infiltration device was placed on top of the box to provide uniformly distributed infiltration ("rain") over the entire surface area of the top of the box. A water-filled reservoir with 64 drips (0.25 mm inner diameter tubing and finger-tight fittings) was connected to a diaphragm pump. The pump rates were tested both before and after each experiment and are listed in Table 1.

Hydrologic Properties

The hydrologic characteristics of the materials were measured separately. The retention characteristics were measured using a dynamic outflow approach, the so-called one-step method (Kool et al., 1985; Parker et al., 1985; Wildenschild et al., 1997) in a smaller pressure cell (7.6 cm diameter, 3.5 cm long). The saturated hydraulic conductivity was measured in a column (2.5 cm diameter, 28 cm long) using the constant head technique (e.g. Klute, 1986). The measured retention curves are shown in Figure 2 and the values listed in Table 2. A non-linear least-squares optimization routine (RETC, vs. 6.0) was used to fit van Genuchten (1980) (VG) parameters to the curves and these parameters are listed in Table 3 and outlined in Figure 3 and 4. As seen in Table 3, the two coarse materials have very similar hydrologic properties, however, the morphology of these two coarse sands was quite different. Evidently, the porosities of the materials vary somewhat between the loose packing of the experimental box and the packing in the smaller pressure cell that was used for the retention curve measurements.

Experimental Results

We are reporting on two experiments using Overton Sand as the fine material and either 8/20 Angular Sand or 2/16 Rounded Sand as the coarse layer. The two experiments are referred to as Experiment 1 and 2, respectively.

Infiltration and outflow rates for the two experiments are shown in Figure 5 and 6. Each figure shows an initial increase in outflow rate until steady-state flow conditions are reached. In addition to infiltration and outflow rates, the average and standard deviations of the outflow rates are outlined in Figures 5 and 6 and listed in Table 1. Apparently, water is being retained in the box in Experiment 1 (Overton over 8/20 Angular Sand); the infiltration rate is higher than the average outflow rate and not within a standard deviation of the latter. The drains are diverting an average of 93.3% of the infiltrating water. In the experiment using the rounded sand as the coarse material (Experiment 2), however, the infiltration rate is within a standard deviation of the outflow rate and the amount of water being withheld in the box is within measurement error. The amount of water being diverted in this case is 99.7%.

The drain suctions and tensiometer readings for the two experiments are shown in Figure 7 and 8. The air-entry value of the lower tensiometer (placed in the coarse material) was exceeded during the initial wetting phase of both experiments and thus no readings are available for the capillary pressure in the coarse material during the experiment. Similarly, the air-entry value of the ceramic plate and of the second drain was exceeded in the first experiment and only one drain was functioning during the experiment. As seen in Figure 7, following the initial adjustment period, the drain pressure was almost constant throughout the experiment (43.2 cm \pm 1.5 cm), whereas the capillary pressure measured at the upper tensiometer (in the fine material) varied somewhat more (32.9 cm \pm 2.8 cm). The more notable capillary pressure fluctuations were closely correlated to temperature variations in the box, illustrated in Figure 9, and are attributed to temperature sensitivity of the transducers. Very similar behavior was observed in the second experiment where both the upper tensiometer and to some degree the drains were influenced by temperature fluctuations, Figure 10. In the second experiment (Figure 8) the upper tensiometer was also fairly constant, apart from temperature induced variations (35.7 cm \pm 2.8 cm). The ceramic plate functioned as an additional tensiometer during part of this experiment and following

the initial non-steady-state wetting period, the measured capillary pressures were almost identical to the capillary pressures measured at the upper tensiometer. After approximately 10 days the ceramic plate ceased to function. The upper tensiometer and the ceramic plate are located at a vertical distance of 21 cm and the fact that practically identical values were measured at both vertical locations indicates that flow had reached steady-state and was driven by gravity alone. The unsaturated hydraulic conductivity is thus equal to the flow rate through the box.

To better illustrate the flow patterns in the experiment, a dye tracer (Phenol Red) was added to the sand surface where it dissolved in the infiltrating water. In the first experiment it was added at the beginning of the experiment (initially dry sand) while in the second experiment it was added after 5 days when the wetting front had already reached the material interface. Phenol Red is a very conservative tracer with low adsorption capabilities. To document the tracer transport we periodically took pictures of the box with a digital camera throughout the experiments. Time-lapse series of photographs for each experiment are shown in Figure 11 and 12 for Experiment 1 and 2, respectively. It is evident from the figures that the water is progressing faster (and further) into the angular sand than into the rounded sand. Also, the dye did not enter a significant distance into the rounded sand, whereas it did follow the water into the angular sand, Figure 13.

At the end of each experiment the box was emptied of sand using an industrial vacuum. Successive layers were carefully removed and samples (app. 25 ml) collected. The samples were weighed and placed in a 105 °C oven over night and subsequently weighed again to determine the water saturation. The measured saturations are listed in Table 4 and their values as a function of sampling location illustrated in Figure 14. As seen in Figure 14, the wetting front had progressed almost 15 cm into the angular sand, whereas only a narrow band of approximately 2 cm were significantly wetted in the rounded material. Since these materials have almost identical hydrological properties, models of capillary barrier performance, which are based on these properties, would predict nearly identical behavior for both experiments. As our experimental results show, such predictions would be inaccurate.

Modeling Studies

Description of Numerical Model

We modeled these experiments with the US1P module of NUFT (Non-isothermal Unsaturated-saturated Flow and Transport) (Nitao, 1998). This module solves the equations for single-phase unsaturated flow in porous media. XTOOL, a NUFT postprocessor code, was used to display the output of the code in graphical form. Both codes were run on a Sun Ultra 10 Workstation. Before simulating the experiments described in this report, we compared the results of a capillary barrier simulation with results reported in Webb (1997) to gain confidence in our ability to model capillary barriers using NUFT. As Fig. 15 shows, the agreement is excellent.

The two-dimensional model domain for the experiments is shown in Fig. 16. The hydrologic properties used in the simulations are given in Table 5. In our numerical model, we describe the relationship between moisture content, capillary pressure (i.e., suction, head) and permeability using the van Genuchten and Mualem expressions (*van Genuchten*, 1980; Mualem, 1976). NUFT input requires different parameters in some cases from those listed in Table 2. For example, NUFT uses the van Genuchten m where $m = 1 - (1/n)$. Also, NUFT uses saturations rather than moisture contents. Saturation, S , is defined as the moisture content, θ , divided by the porosity, ϕ . We assume that $\theta = \phi$ in our simulations.

Initially, the sands are assumed to be completely dry. The top boundary and the drain are held at constant head and saturation. The infiltration rate and drain suction used in the simulations are given in Table 5. The grid shown in Fig. 16 is the one used for the results presented here. Simulations for Experiment 1 were done with approximately double the grid resolution with no significant difference in model results. Simulations for Experiment 1 and 2 were run out to 33 days and 18 days, respectively, to match the actual length of the laboratory experiments.

Model Results

The saturation fields for Experiments 1 and 2 using the domain and grid shown in Fig. 16 and the parameter values given in Table 5 are shown in Fig. 17. As these figures clearly show, NUFT predicts successful performance of the barrier, and the complete absence of any wetting front into the lower coarse material in both cases.

Since these simulation results did not match our laboratory results, we tried adjusting hydrologic parameters determined in the laboratory to achieve a better match. We used two principles to guide us with respect to which parameters we adjusted and by how much. The first was the likely bounds of general parameter uncertainty. The second was the likely differences between the parameters determined from the drying curves we used to determine the values reported in Table 5 and the parameters values that we would have determined had we measured wetting curves rather than drying curves. In general, a wetting curve has a similar van Genuchten n -value but a greater α -value. For these experiments, wetting curves more likely represent the conditions in the coarse sand. For the fine sand, it is more difficult to know which curve better represents conditions in the system; most likely the most representative values are somewhere in between those for the two curves.

A systematic parameter adjustment study was not performed due to time constraints, but as Fig. 18 shows, we were able to simulate the movement of the wetting fronts into the lower

coarse sands as observed in the laboratory experiments by using the adjusted hydrologic parameters as listed in Table 6. These adjustments are well within the bounds of parameter uncertainty as discussed above.

We also performed a much longer-term simulation of Experiment I with the adjusted parameters. The results, shown in Fig. 19, show that while the saturation in the coarse lower layer approaches a steady-state in less than 1 year, the flux of water through the layer toward the drain appears to continue.

Discussion and Conclusion

We have performed two capillary barrier experiments using almost identical initial and boundary conditions, but using different coarse materials. The coarse materials have very similar hydrologic properties, but are morphologically different. The rounded sand provided a better functioning capillary barrier than the angular sand, but neither of the materials (in combination with the Overton Sand) provided a perfectly working capillary barrier. Our measurements of hydrologic parameters are typical of those routinely done for studies of unsaturated flow in porous materials. Our experimental results therefore indicate that prediction of capillary barrier performance based on standard hydrologic property parameter measurements is not always adequate to predict system behavior. We believe this is an important point to consider with respect to capillary barrier design.

Our numerical simulations predicted that for the measured material properties, the barriers should be functioning perfectly, with no infiltration into the coarse layer. The numerical simulations were very sensitive to small changes in hydrologic properties. When slightly different hydrologic parameters were used in the numerical model, we were able to simulate the behavior observed in the experiments. This also supports the point that prediction of capillary barrier performance based on standard hydrologic property parameter measurements is not always adequate to predict system behavior,

Success or failure? - Regardless of the fact that water infiltrated the lower coarse material in both our experiments, it is important to keep in mind that the majority of the water was diverted by the drains in both cases (93.3% for the angular sand and 99.7% for the rounded sand). Our (very limited) numerical modeling results suggest that the system would eventually reach a steady-state, with a partially saturated coarse layer and a low but steady flux of water through at least a part of that layer. The question then arises whether this should be deemed adequate to consider the capillary barrier a success. The answer to this question depends on the performance goals for the system.

These experiments and associated modeling efforts are the first step in better understanding capillary barriers as they might be used in an engineered barrier system at the potential high-level nuclear waste site at Yucca Mountain. There are many questions that remain to be investigated, including the role of various infiltration scenarios, the relative position and suction level of drains, and the role of thermohydrologic processes.

References

Klute, A. (ed.), 1986. *Methods of soil analysis. Part 1. 2nd. ed.*, Agron. Monogr., 9, ASA and SSSA, Madison, WI.

- Kool, J.B., J.C. Parker, and M.Th. van Genuchten, 1985. Determining soil hydraulic properties from one-step outflow experiments by parameter estimation: 1. Theory and numerical studies. *Soil Sci. Soc. Am. J.*, 49, 1348-1354.
- Mualem, Y. (1976), A new model for predicting the hydraulic conductivity of unsaturated porous materials, *Water Resources Research* 12, 513-522.
- Nitao, J.J. 1998. *Reference Manual for the NUFT Flow and Transport Code, Version 2.0.* UCRL-MA-130651. Livermore, California: Lawrence Livermore National Laboratory.
- Oldenburg, C. M. and Pruess, K. (1993), *On numerical modeling of capillary barriers*, *Water Resources Research*, 29(4), p. 1045-1056.
- Parker, J.B., J.C. Kool, and M. Th. van Genuchten, 1985. Determining soil hydraulic properties from one-step outflow experiments by parameter estimation: 2. Experimental studies. *Soil Sci. Soc. Am. J.*, 49, 1354-1359.
- van Genuchten, M. Th. 1980. A closed-form equation for predicting the hydraulic conductivity of unsaturated soils. *Soil Sci. Soc. Am. J.* 44:892-898.
- Webb, S.W. (1997) Generalization of Ross' tilted capillary barrier diversion formula for different two-phase characteristic curves, *Water Resources Research*, 33(8), p. 1855-1859.
- Wildenschild, D., K. H. Jensen, K.J. Hollenbeck, T.H. Illangasekare, D. Znidarcic, T. Sonnenborg and M.B. Butts, 1997. A two-stage procedure for determining unsaturated hydraulic characteristics using a syringe pump and outflow observations. *Soil Sci. Soc. Am. J.*, 61(2), 347-359.

Table 1.Material properties and boundary conditions for the experiments.

	Experiment 1 Overton over 8/20 angular sand	Experiment 2 Overton over 2/16 rounded sand
porosity of fine layer	0.39	0.44
porosity of coarse layer	0.50	0.41
pump rate (ml/h)	29.8	29.3
pump rate (m/s)	$1.37 \cdot 10^{-7}$	$1.35 \cdot 10^{-7}$
average outflow rate (ml/h)	27.8 +/- 0.8	29.2 +/- 1.3
average drain suction (cm)	43.2 +/-1.5	46.3 +/- 2.1

Table 2. Measured retention data for the three sands.

Overton Sand		2/16 Rounded Sand		8/20 Angular Sand	
capillary pressure	capillary water content	pressure	water content	capillary pressure	water content
cm		cm		cm	
0	0.3264377	0	0.3394377	0	0.439546
56.4685	0.3113469	14.0505	0.3339756	10.9635	0.4222471
55.4155	0.3082926	12.962	0.3281324	10.894	0.4175988
54.2655	0.3048561	12.775	0.3223381	10.8945	0.413017
53.891	0.3017515	12.8765	0.3162458	10.9645	0.4086341
53.6645	0.2986137	12.935	0.3107339	10.932	0.4040027
53.165	0.2955927	13.0575	0.3042926	11.418	0.3729246
52.8865	0.292687	13.1485	0.2984155	11.824	0.3350916
53.157	0.2899145	13.2715	0.2922899	11.6155	0.3308418
53.177	0.2869932	13.4425	0.286778	11.925	0.3271555
53.224	0.2842702	13.4	0.2810177	12.0105	0.3236864
53.4625	0.28178	13.517	0.2756884	12.315	0.3005295
55.461	0.2788248	13.64	0.2711921	12.5935	0.283279
53.1915	0.2765343	13.5385	0.2653944	12.861	0.2674406
53.5815	0.2736124	13.6825	0.2598683	13.1595	0.255852
54.1165	0.2711222	13.752	0.2541589	13.341	0.2466735
54.443	0.2649464	13.768	0.2485309	13.5385	0.2413103
57.6765	0.2603781	13.886	0.2426653	13.7465	0.2393347
57.946	0.2582396	13.849	0.237241	13.784	0.2388663
57.816	0.2560672	13.88	0.2317284	14.2855	0.2312831
58.04	0.2540034	13.95	0.226148	15.541	0.218683
58.3655	0.251797	14.1685	0.2211514	17.0415	0.2107604
58.6455	0.2501066	14.201	0.2154895	19.0445	0.2028106
58.7535	0.2477644	14.334	0.2102145	21.0365	0.1990563
58.6405	0.2458703	14.2965	0.2049667	23.0765	0.1977461
58.779	0.2439762	14.27	0.1996578	25.005	0.1955872
57.742	0.2419396	14.3665	0.1946069	27.002	0.1949287
57.847	0.2402627	14.6865	0.1899566	29.0415	0.1946096
58.16	0.2383007	14.564	0.1846137	31.0125	0.1936117
59.752	0.2365085	14.799	0.1803164	33.058	0.1938493
57.48	0.2348316	14.922	0.1752179	35.0125	0.1930686
58.8485	0.2329375	14.858	0.1710156	37.1545	0.1929328
58.2	0.23141	14.8145	0.1672682	39.002	0.1930007
59.562	0.2297196	15.012	0.163446	41.12785	0.1930482
59.4925	0.2280224	15.2735	0.160296	43.1302	0.1926001

59.1745	0.2267325	15.349	0.1570238	45.0214	0.1925051
60.891	0.224757	15.349	0.154186	47.02955	0.1926816
60.116	0.2231752	15.381	0.1518914	49.079955	0.193313
60.2295	0.2217834	15.4345	0.149203	51.04485	0.1933333
60.146	0.2203238	15.6045	0.1467454	52.27315	0.1928174
60.279	0.218742	15.7385	0.1453537	53.02075	0.1927155
60.7075	0.2172485	15.728	0.1429097	54.01425	0.1932994
60.692	0.2158907	15.6105	0.1409681	55.087835	0.1926205
60.9635	0.2132023	15.626	0.1390604	57.20779	0.1926544
61.094	0.2109416	15.755	0.1377162		
61.22	0.2079341	15.861	0.1362363		
61.623	0.2055988	15.8455	0.1349599		
61.8105	0.2036707	16.07	0.1335954		
63.1065	0.1921161	15.99	0.1324005		
63.363	0.1903103	16.107	0.1321018		
63.397	0.1887284	16.2945	0.130907		
63.439	0.1867393	16.2835	0.12978		
66.6385	0.148518	16.267	0.1288975		
68.588	0.1294616	16.214	0.1281711		
70.7495	0.112184	16.3905	0.1275058		
72.687	0.0998486	16.924	0.121294		
74.0365	0.0917291	17.149	0.1170441		
76.2255	0.0841256	18.126	0.111002		
78.383	0.0765221	18.6915	0.1056253		
80.615	0.0707923	19.0235	0.1036972		
82.087	0.0672892	19.4075	0.1011446		
84.685	0.0632906	19.9575	0.0990333		
86.584	0.0604528	248.625	0.0960597		
88.6125	0.0584908				
90.6266	0.0566307				
98.691735	0.0544718				
100.4887	0.0545058				
110.7455	0.0550421				

Table 3. Material hydrologic properties.

	α (cm ⁻¹)	n	θ_s	θ_r	K_s (m/s)
Overton sand	0.016	10.9	0.33	0.06	$5.3 \cdot 10^{-5}$
8/20 angular sand	0.083	15.3	0.44	0.2	$1.2 \cdot 10^{-4}$
2/16 rounded sand	0.071	16.6	0.34	0.096	$1.4 \cdot 10^{-4}$

Table 4. Saturation as a function of distance from the material interface.

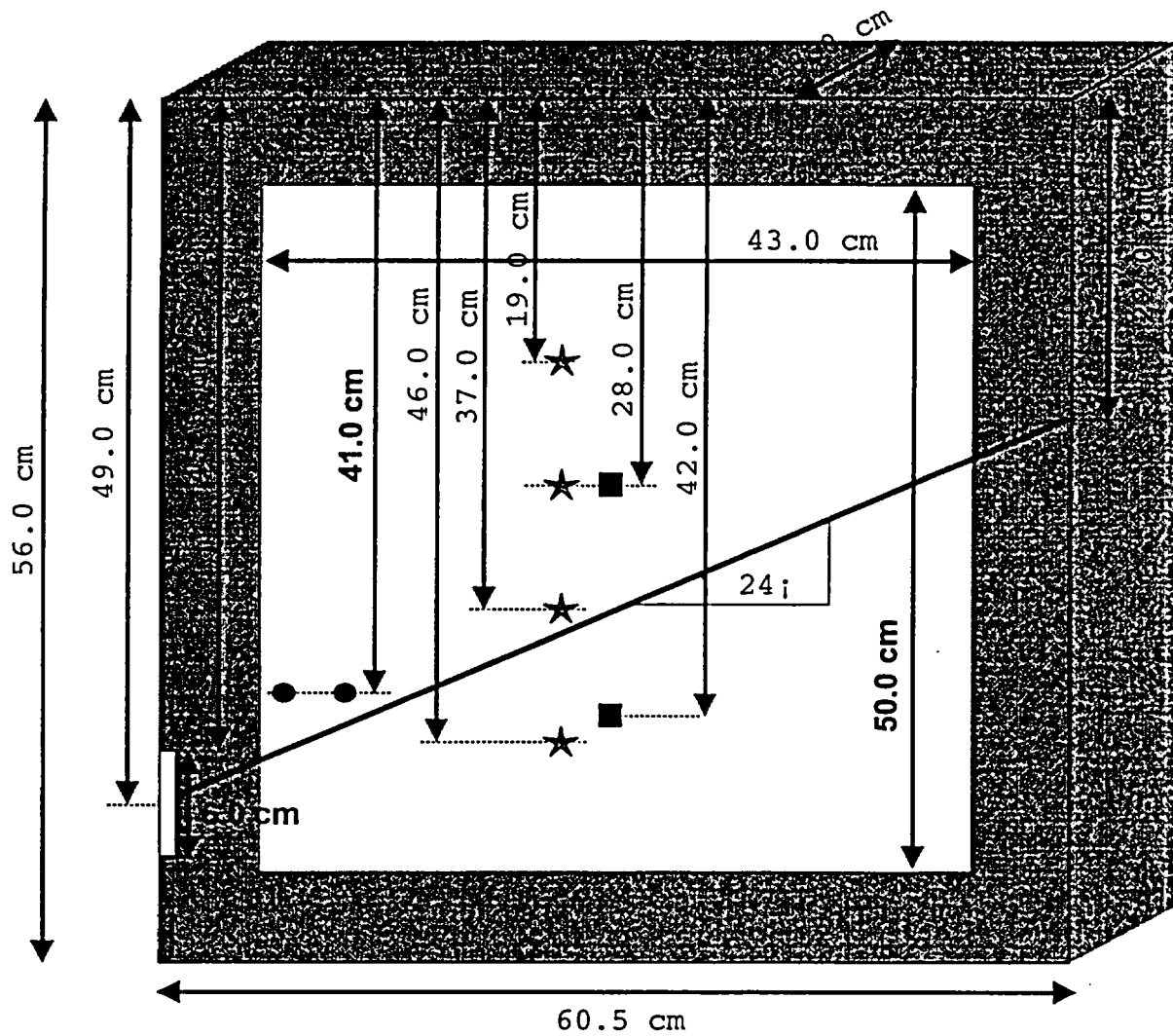
Experiment 1		Experiment 2	
distance from interface (cm)	S_w	distance from interface (cm)	S_w
0	0.338	0	0.289
2.5	0.330	2.9	0.049
6.2	0.308	6.4	0.036
9.9	0.267		
13.2	0.108		

Table 5. NUFT base input parameters

	Experiment 1 Fine = Overton Coarse = 8/20 angular	Experiment 2 Fine = Overton Coarse = 2/16 rounded
Infiltration rate (m/s)	1.37e-7	1.35e-7
Drain suction (m)	0.432	0.463
<i>Fine sand:</i>		
K_s (m/s)	5.3e-5	5.3e-5
α (m ⁻¹)	1.6	1.6
m	0.91	0.91
S_r	0.18	0.18
ϕ	0.33	0.33
<i>Coarse sand:</i>		
K_s (m/s)	1.2e-4	1.4e-4
α (m ⁻¹)	8.3	7.1
m	0.93	0.94
S_r	0.45	0.28
ϕ	0.44	0.34

Table 6. NUFT adjusted input parameters

	Experiment 1 Fine = Overton Coarse = 8/20 angular		Experiment 2 Fine = Overton Coarse = 2/16 rounded	
	Table 5 values	adjusted values	Table 5 values	adjusted values
<i>Fine sand:</i>				
K_s (m/s)	5.3e-5	2e-5	5.3e-5	2e-5
α (m ⁻¹)	1.6	3.2	1.6	3.2
<i>Coarse sand:</i>				
K_s (m/s)	1.2e-4	6.e-5	1.4e-4	1.e-4
m	0.93	0.75	0.94	0.8
ϕ	0.44	0.5		



- tensiometers (porous ceramic cups)
- drainage ports (sintered stainless steel rods)
- ★ thermocouples

Figure 1. Experimental setup.

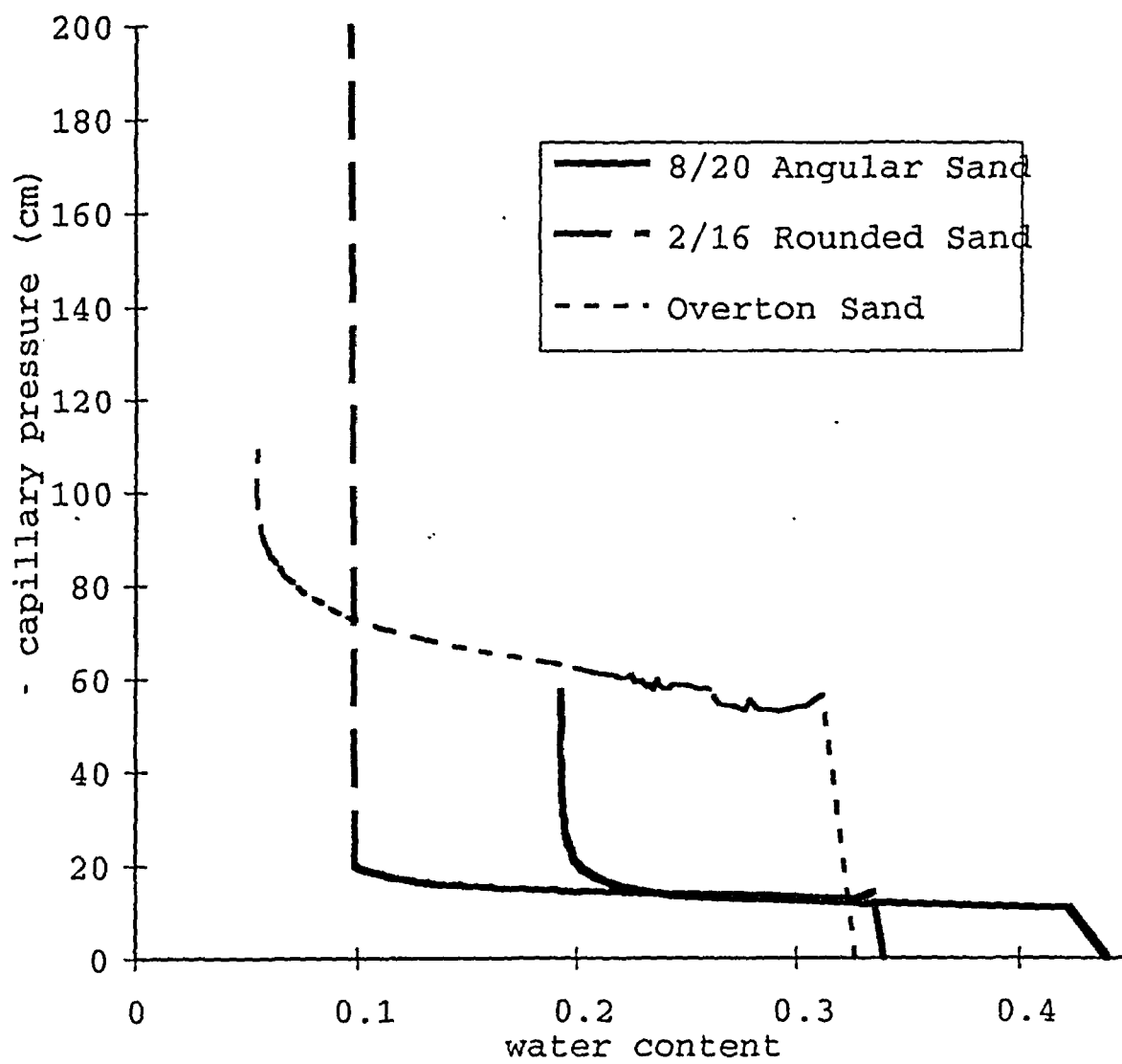


Figure 2. Measured retention characteristics for the three materials.

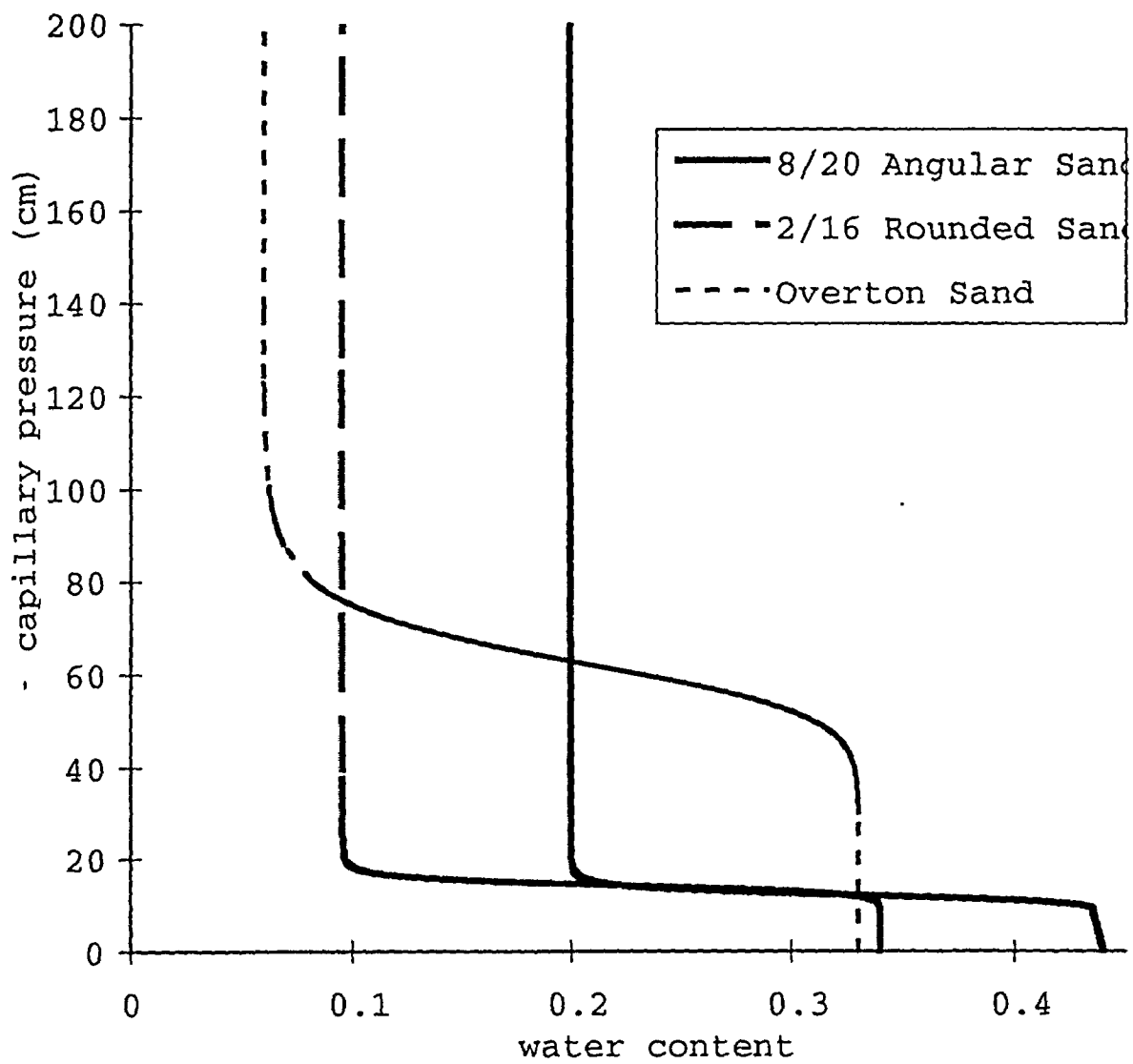


Figure 3. Fitted retention characteristics for the three materials (using RETC).

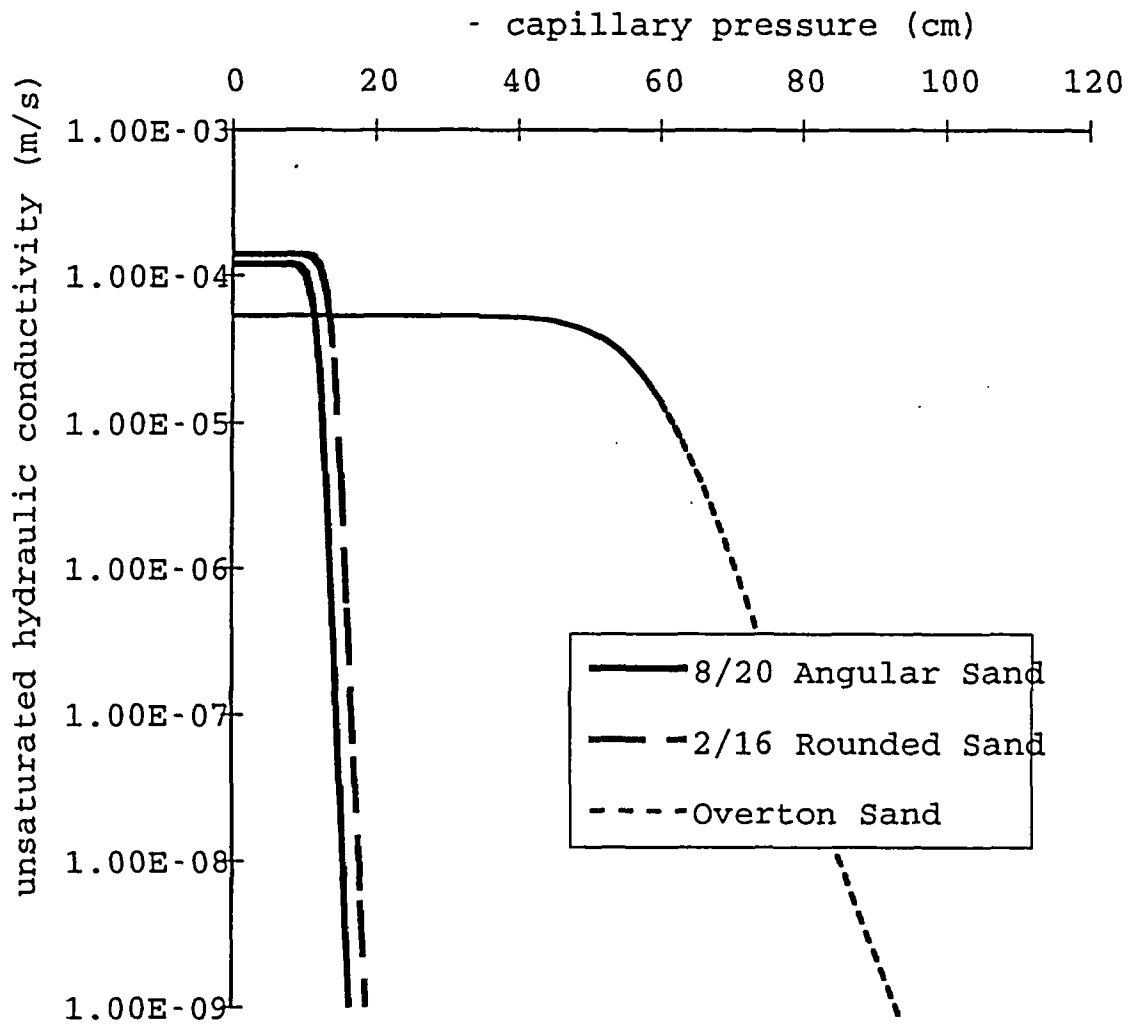


Figure 4. Hydraulic conductivity characteristics for the three materials (based on fitted VG -parameters).

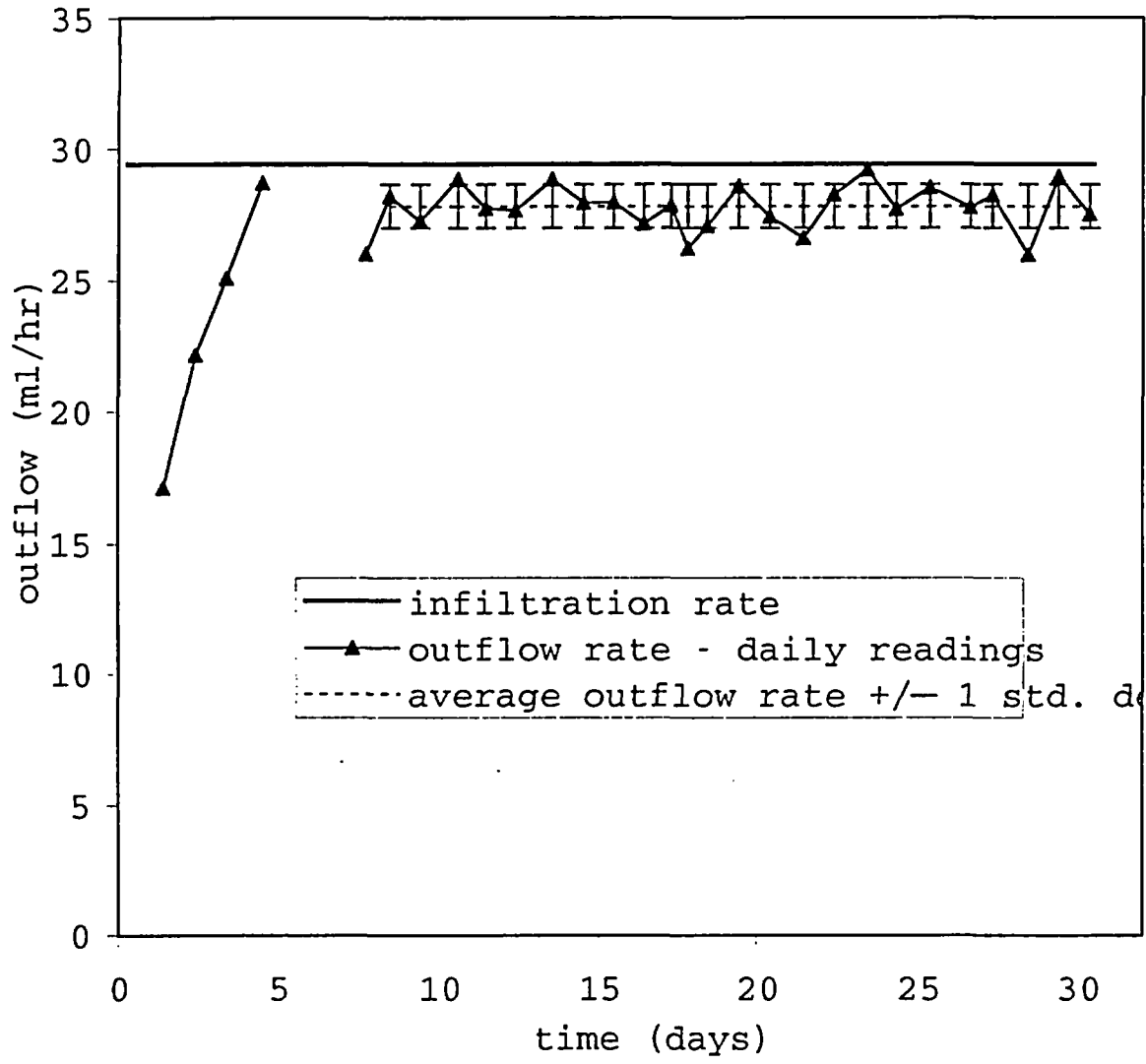


Figure 5. Water balance for Experiment 1 (Overton over 8/20 angular sand)

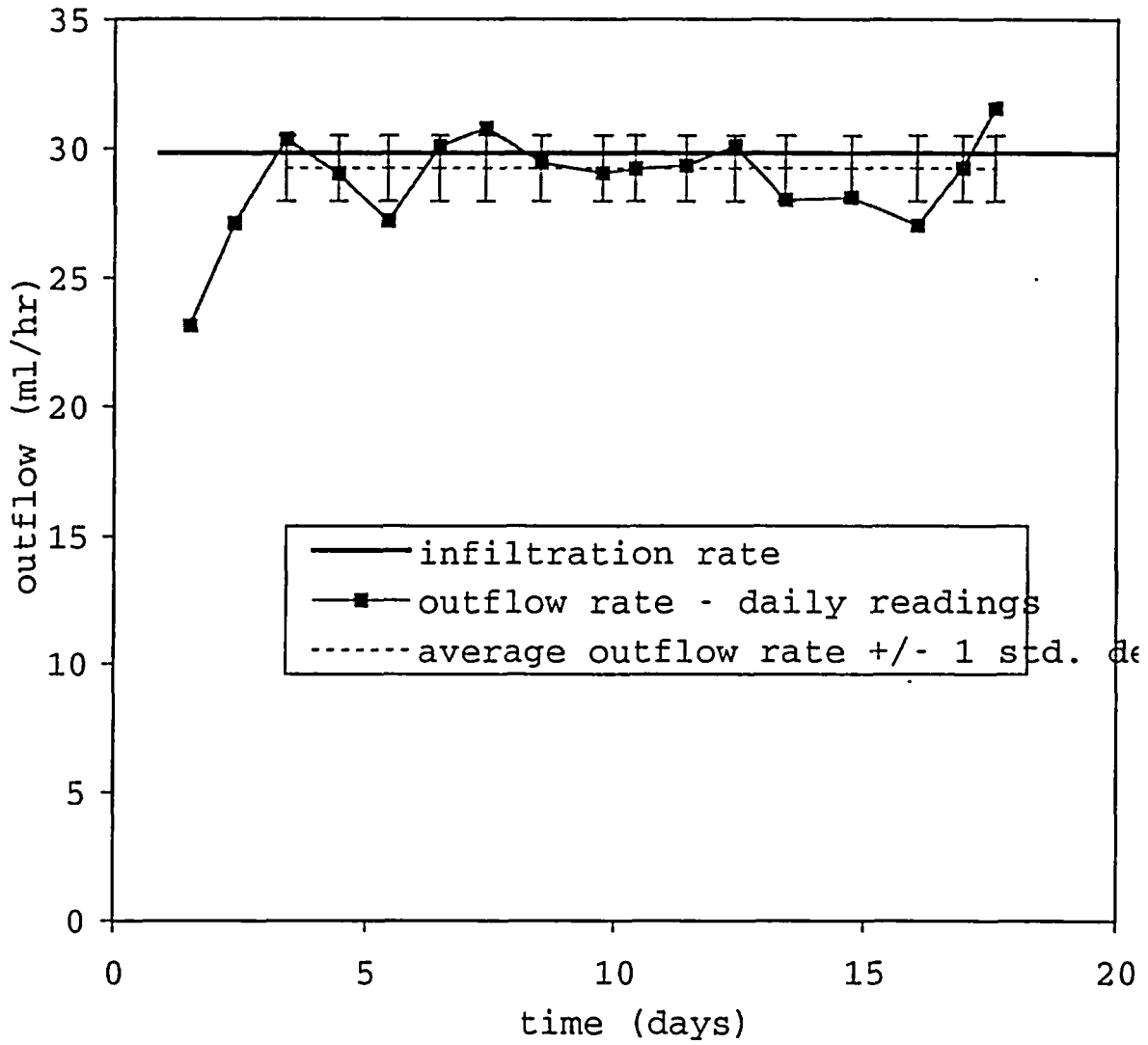


Figure 6. Water balance for Experiment 2 (Overton over 2/16 rounded sand).

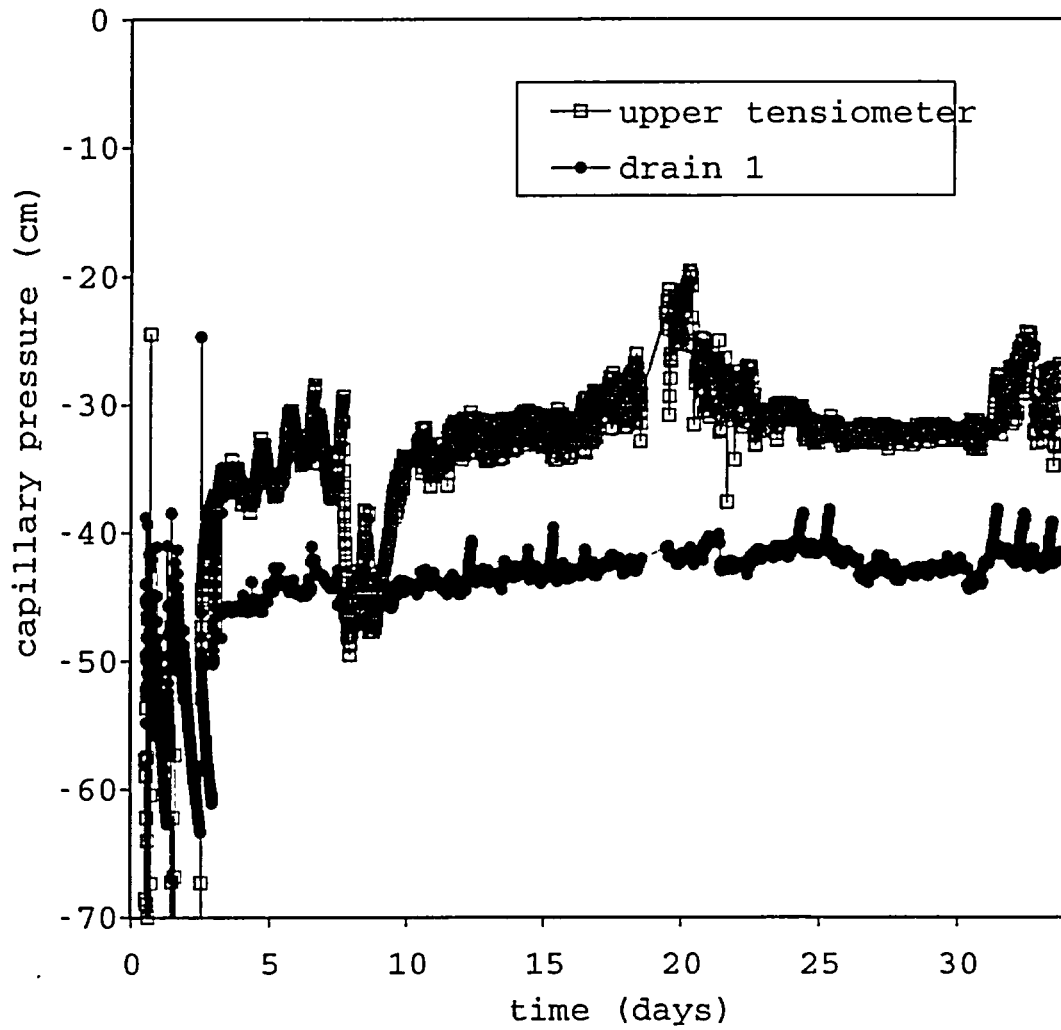


Figure 7. Tensiometer and drain pressures for Experiment 1. The lower tensiometer, the ceramic plate, and the second drain were not operable during this experiment (the air-entry values were exceeded).

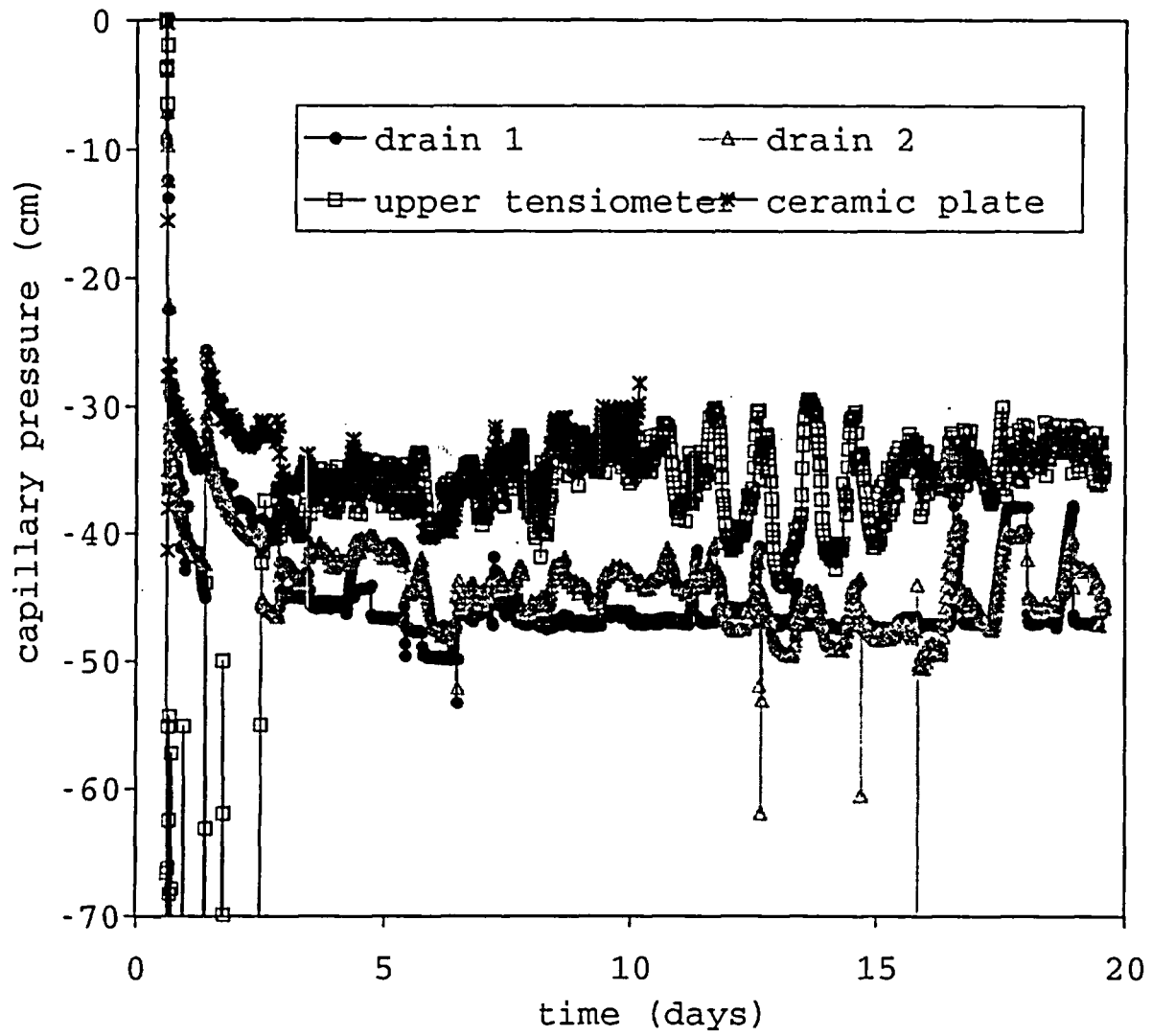


Figure 8. Tensiometer and drain pressures for Experiment 2. The ceramic plate functioned as an additional tensiometer in the fine material for this experiment.

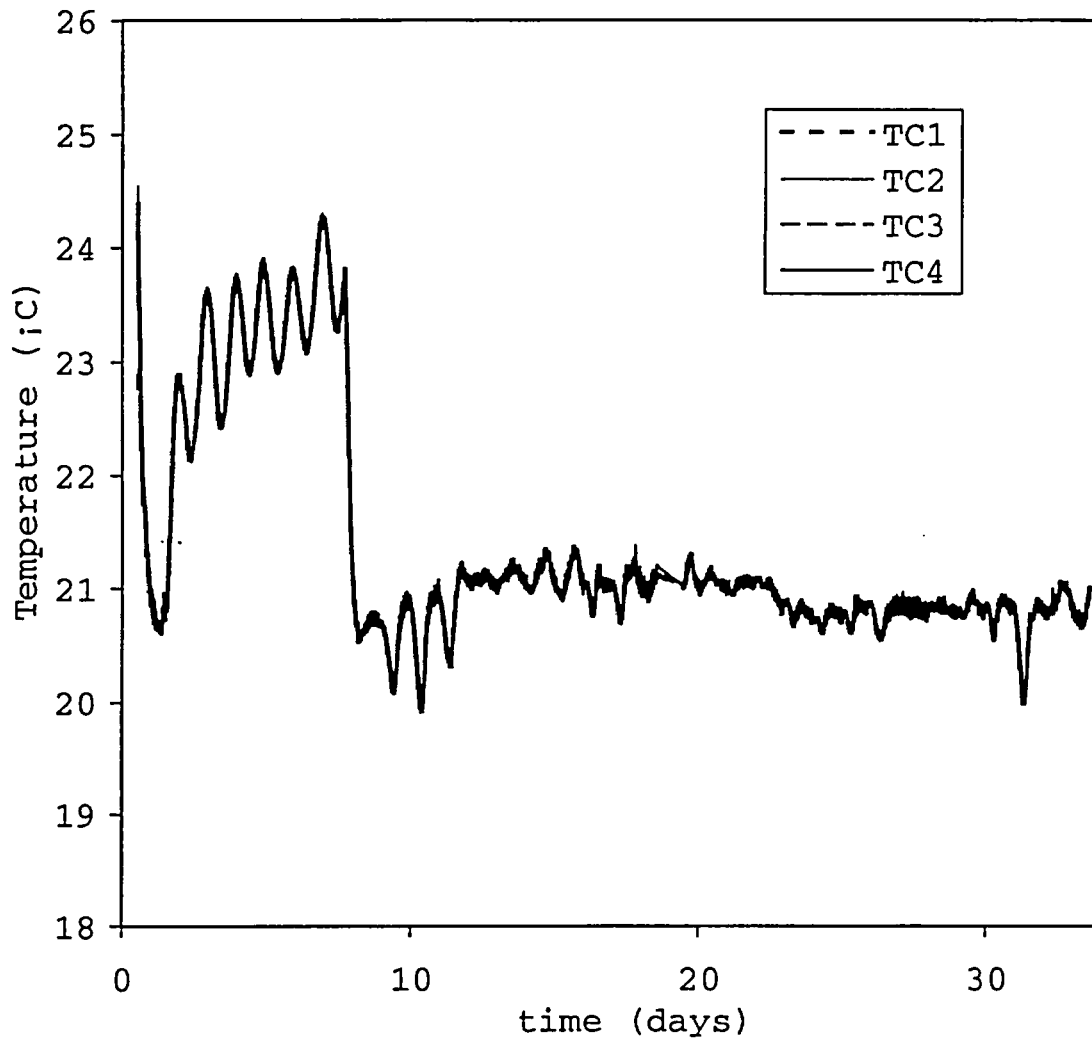


Figure 9. Temperature in the box during Experiment 1 measured with four thermocouples (distance from top; TC1 = 19 cm, TC2 = 28 cm, TC3 = 37 cm, TC4 = 46 cm, details in Figure 1)

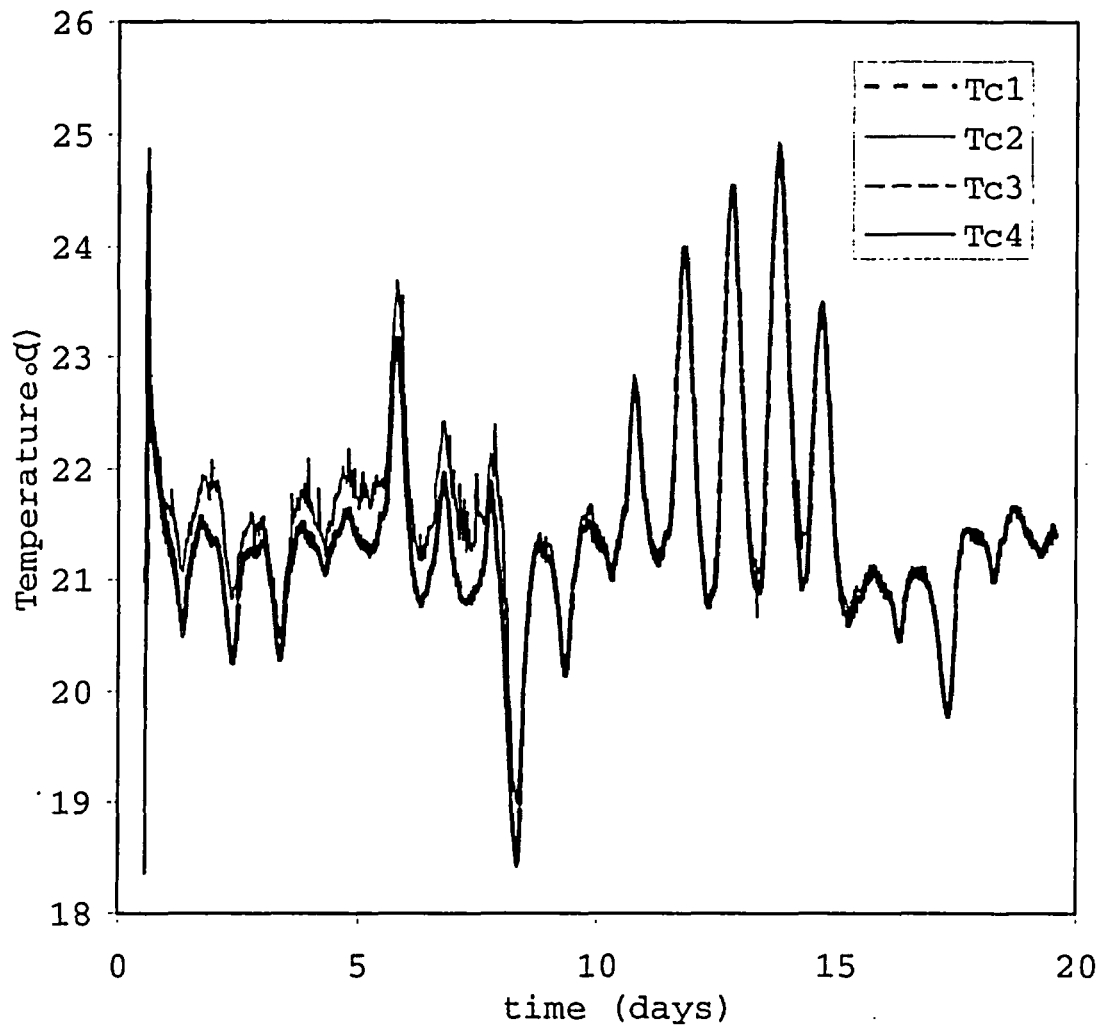


Figure 10. Temperature in the box during Experiment 2 measured with four thermocouples placed as described in Figure 8.

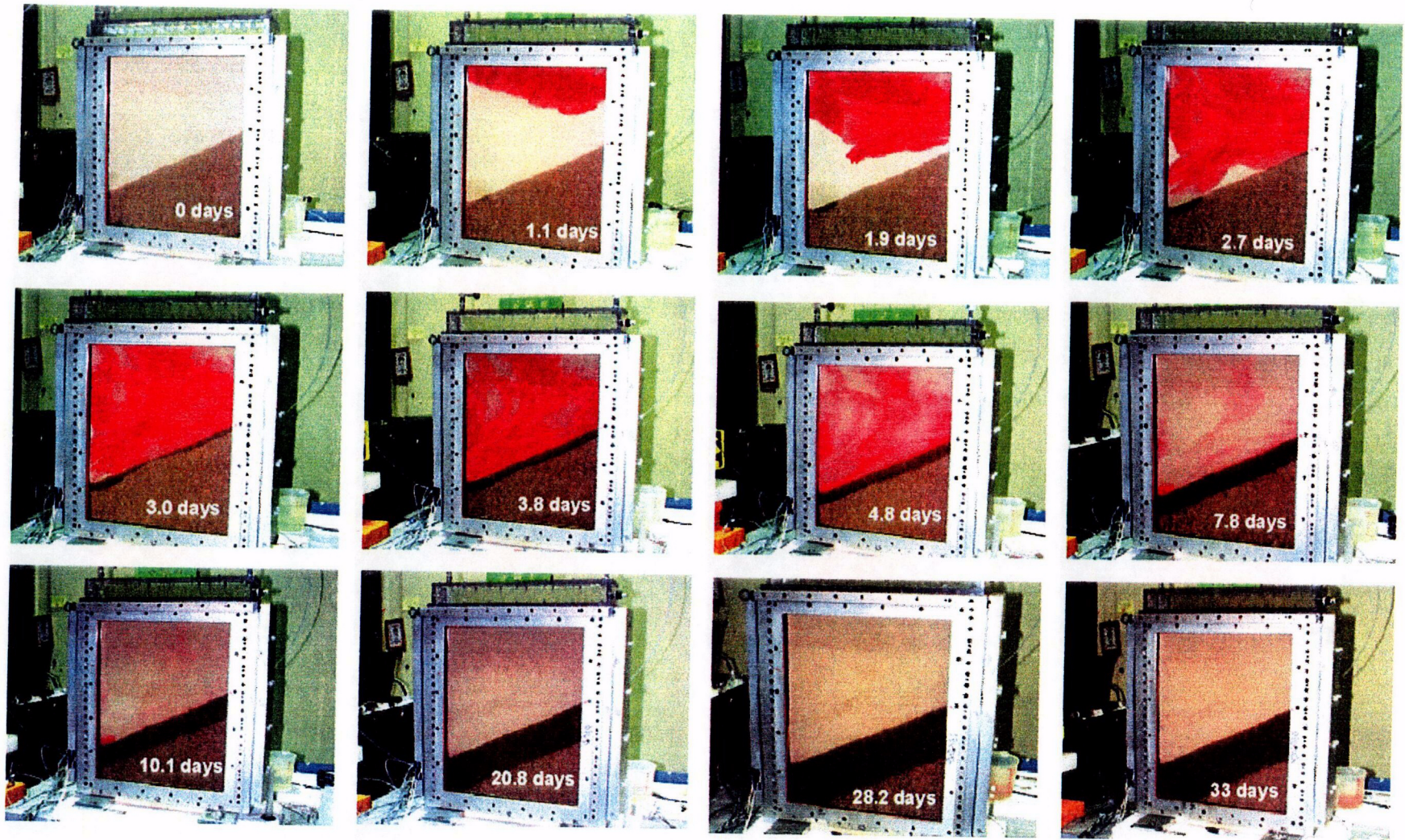


Figure 11. Dye tracer transport time-lapse for Experiment 1 (Overton over 8/20 Angular Sand).

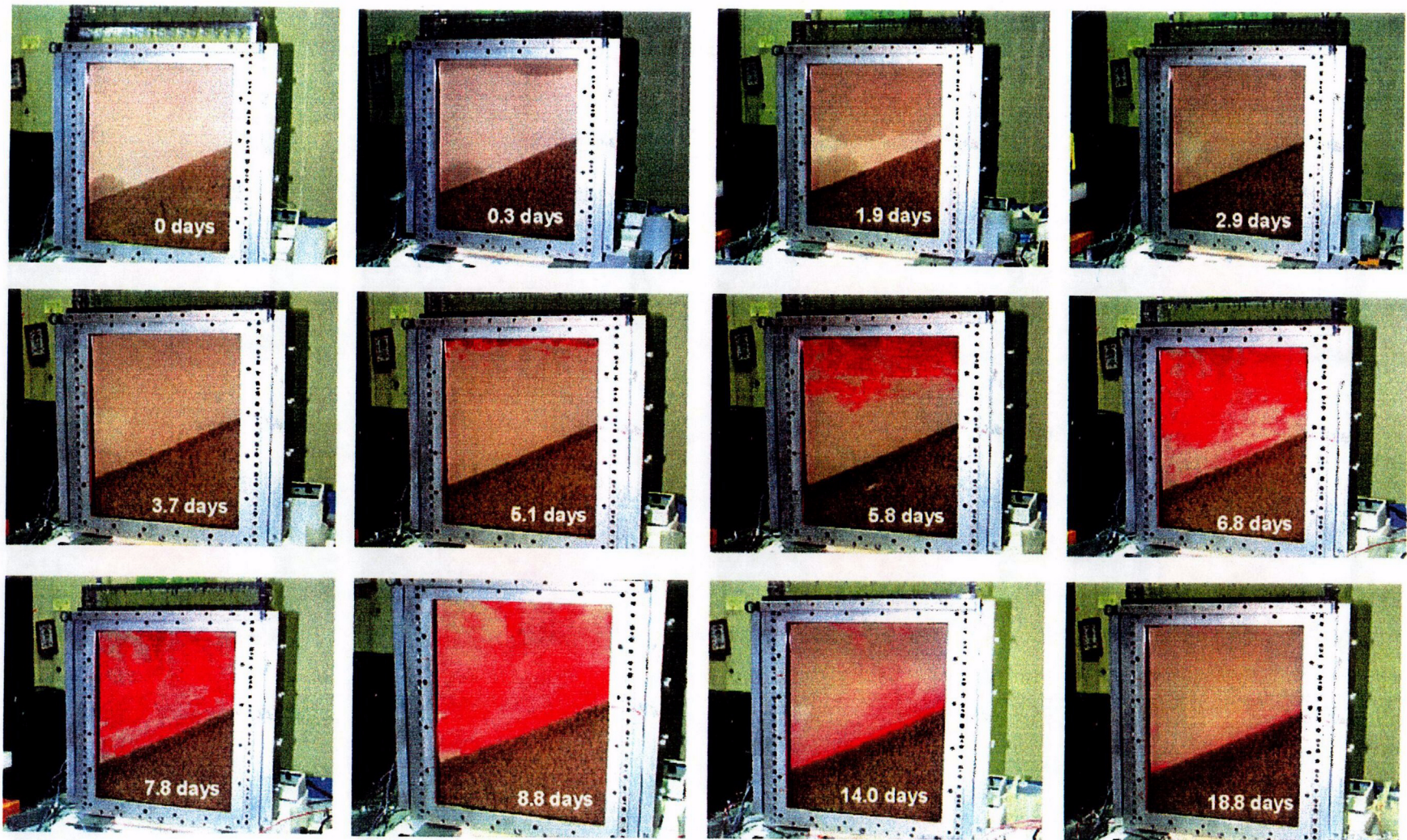


Figure 12. Dye tracer transport time-lapse for Experiment 2 (Overton over 2/16 Rounded Sand).

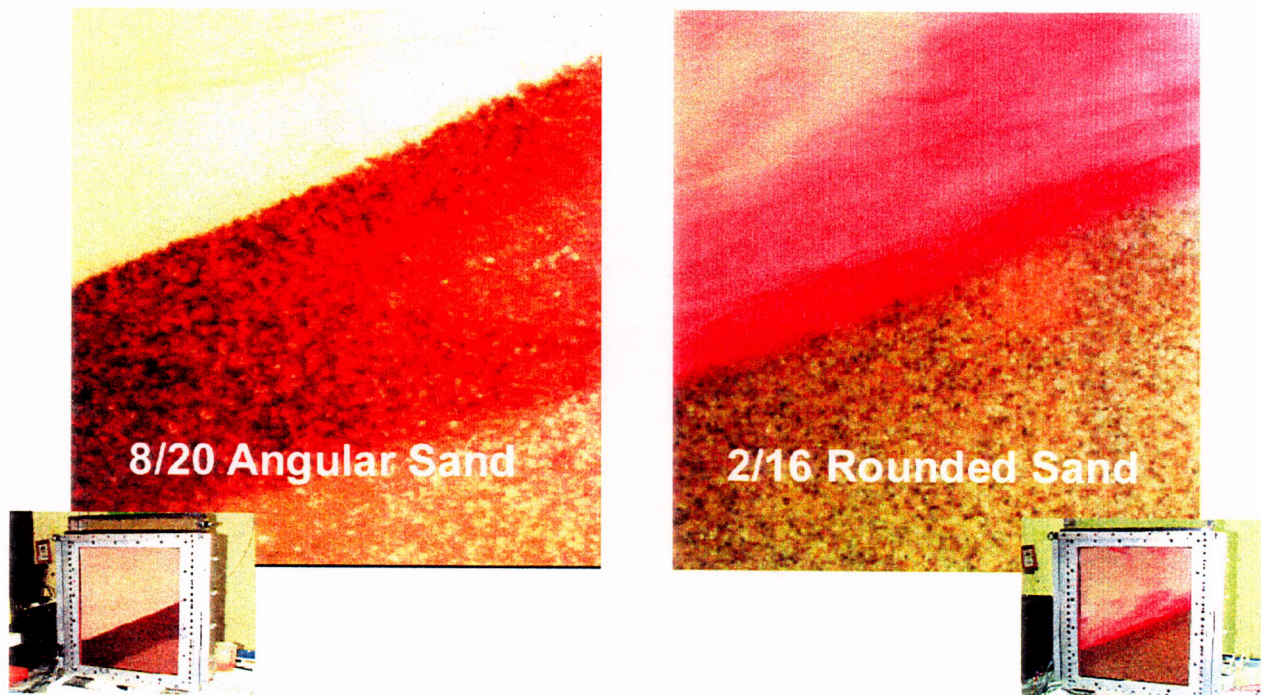


Figure 13. Dye penetration into the coarse material for the two experiments.

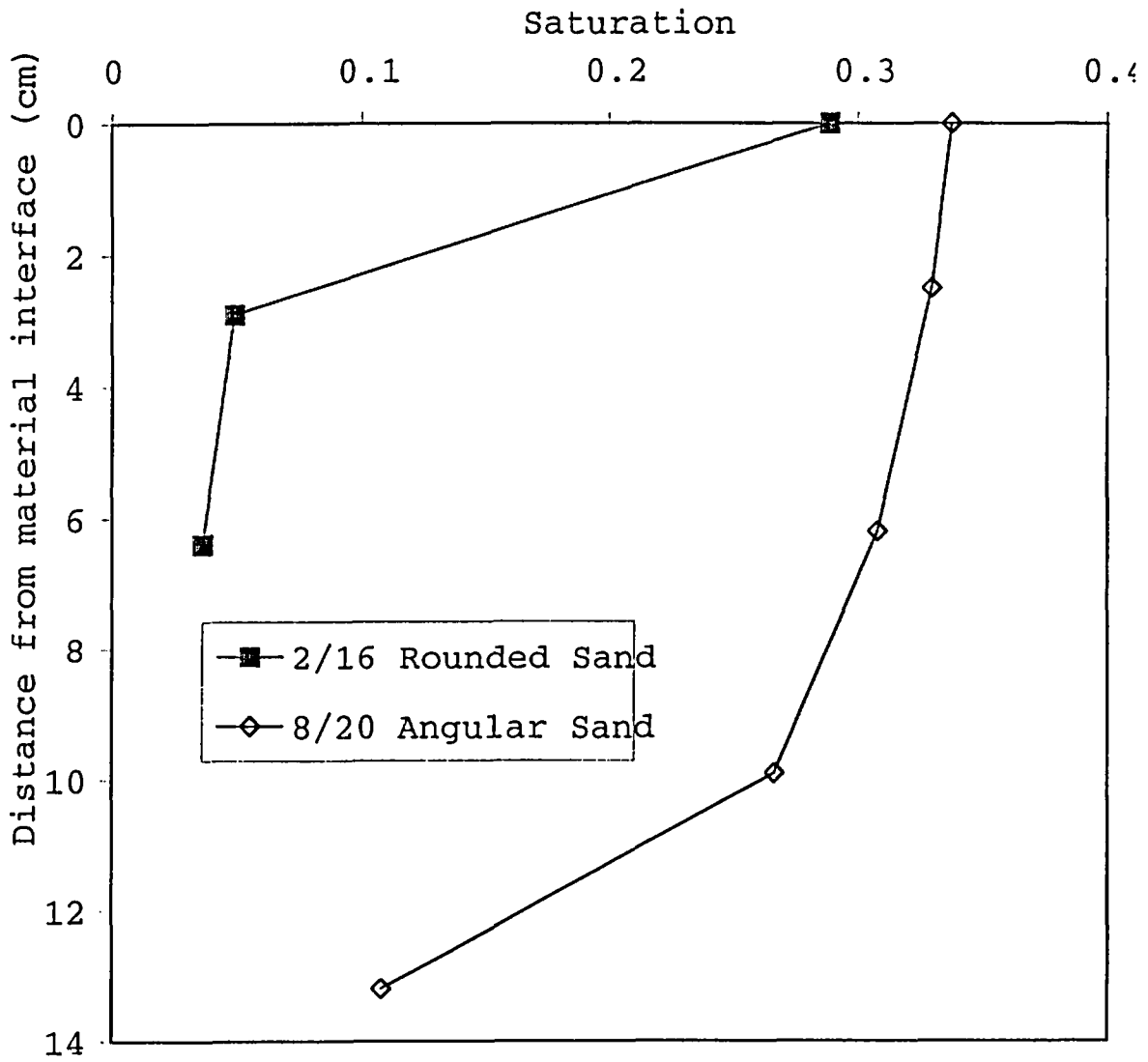


Figure 14. Saturation as a function of distance from the material interface.

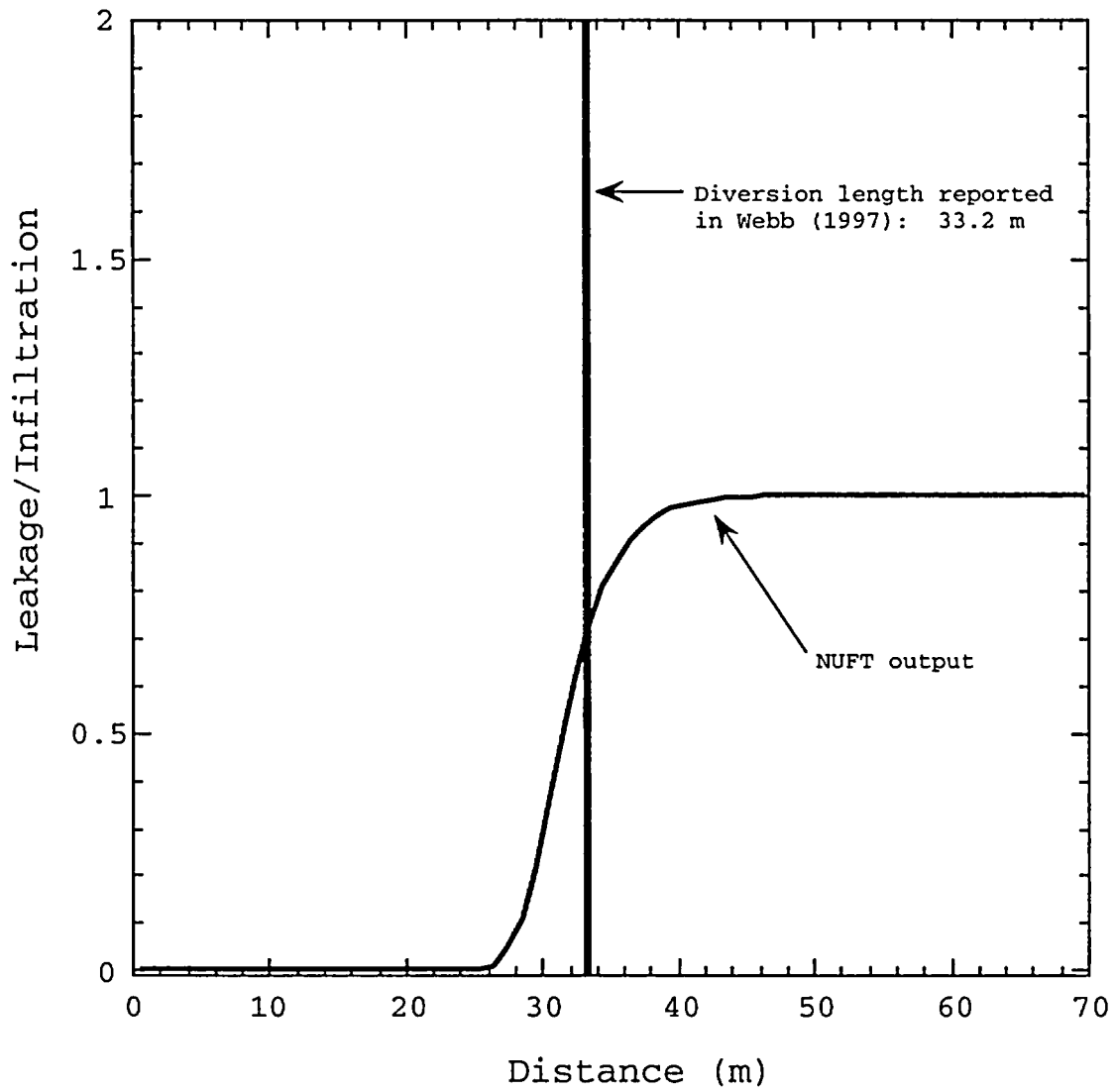


Figure 15. Comparison of NUFT numerical simulation results with the prediction based on analytical relationship, as reported in Webb (1997).

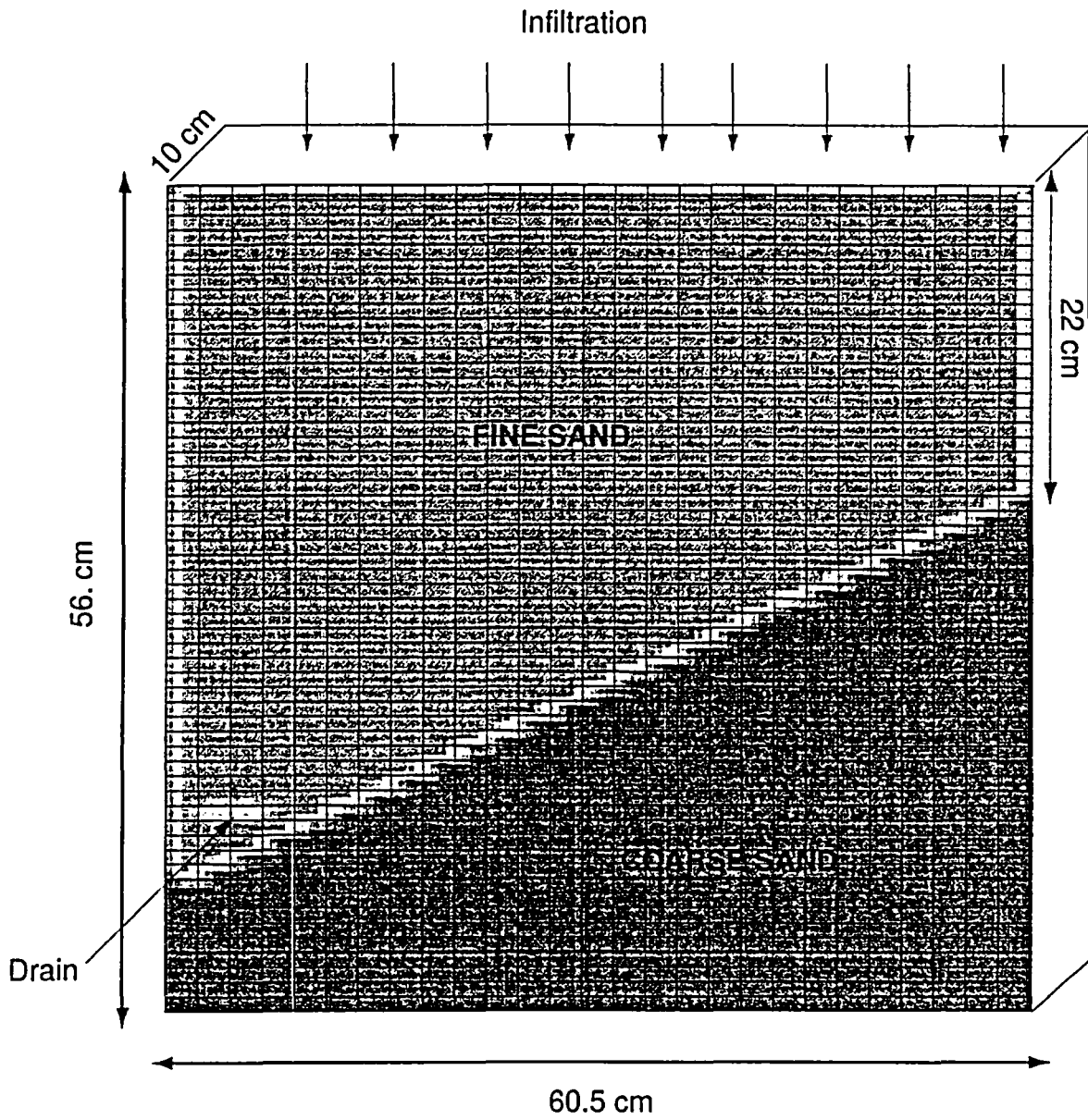


Figure 16. Model domain used in NUFT simulations of laboratory experiments.

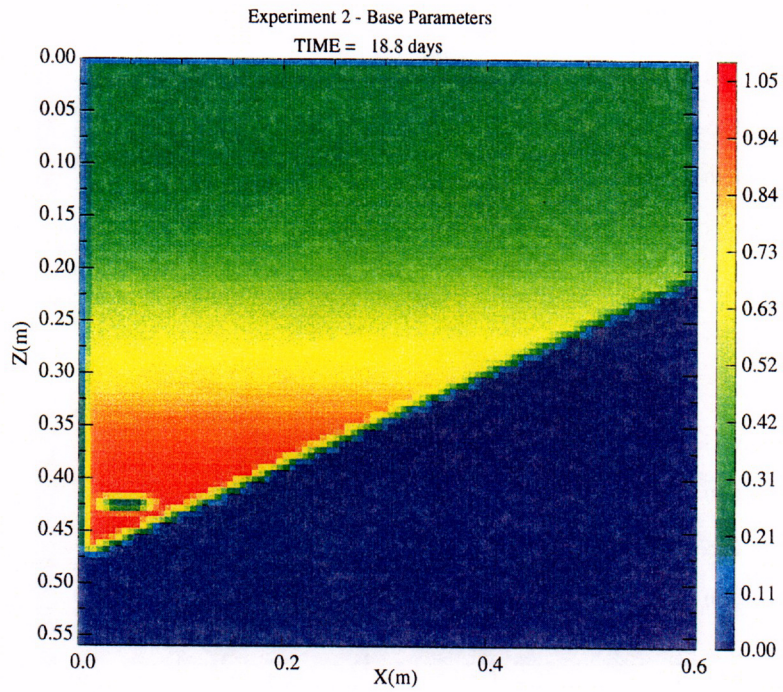
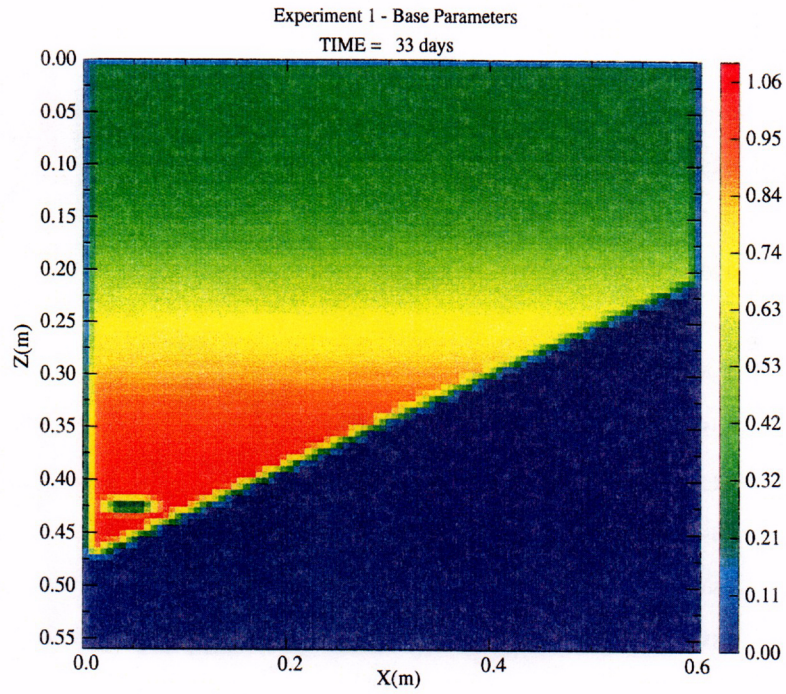


Figure 17. Simulated saturation fields for Experiments 1 and 2 using the base parameters given in Table 5.

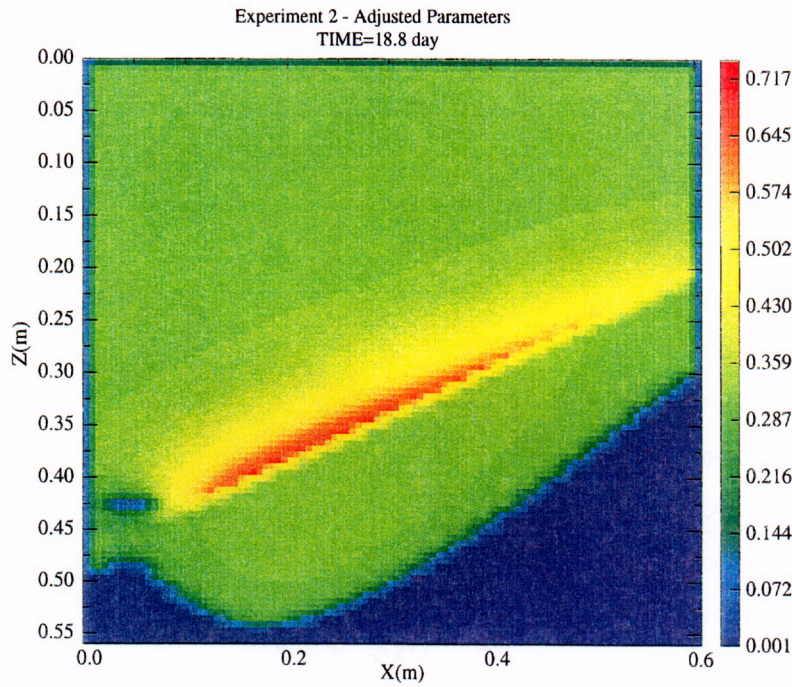
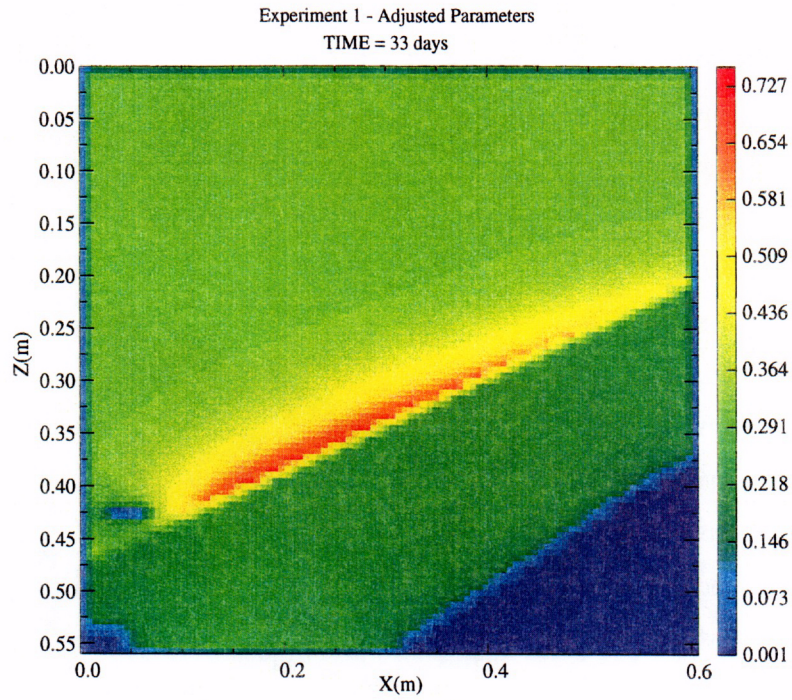
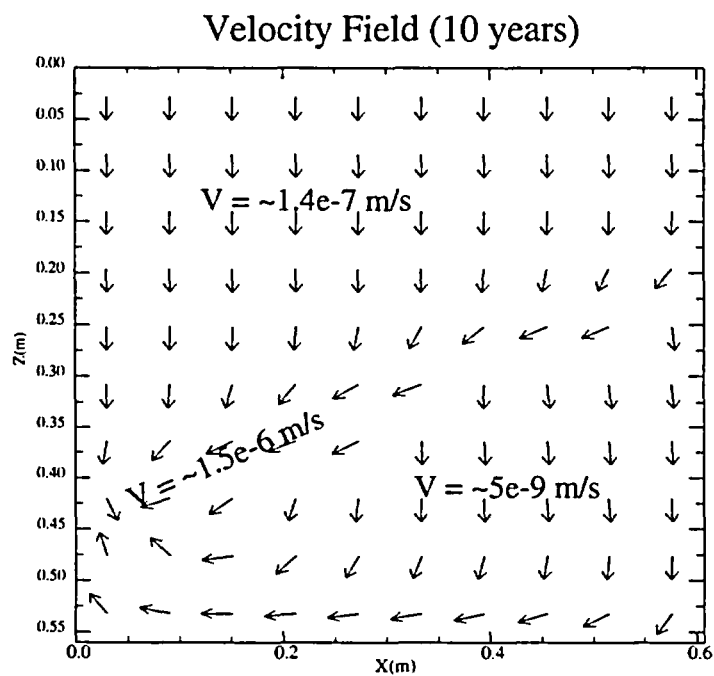
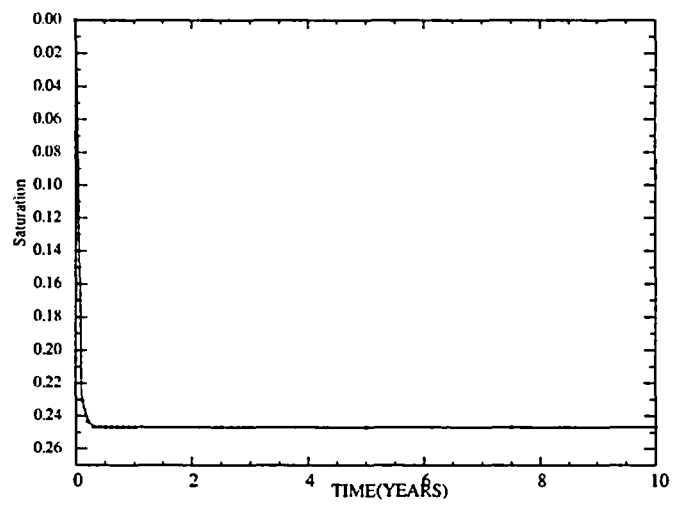


Figure 18. Simulated saturation fields for Experiments 1 and 2 using the adjusted parameters given in Table 6.



Experiment 1 - Adjusted Parameters

Figure 19. Results of 10 years simulation of Experiment 1 with adjusted parameters as given in Table 6.

Technical Information Department · Lawrence Livermore National Laboratory
University of California · Livermore, California 94551

